



Pulmonary inflammation following intratracheal instillation of cellulose nanofibrils in rats: comparison with multi-walled carbon nanotubes

Katsuhide Fujita · Sawae Obara · Junko Maru · Shigehisa Endoh

Received: 12 March 2021 / Accepted: 11 May 2021 / Published online: 28 May 2021
© The Author(s) 2021

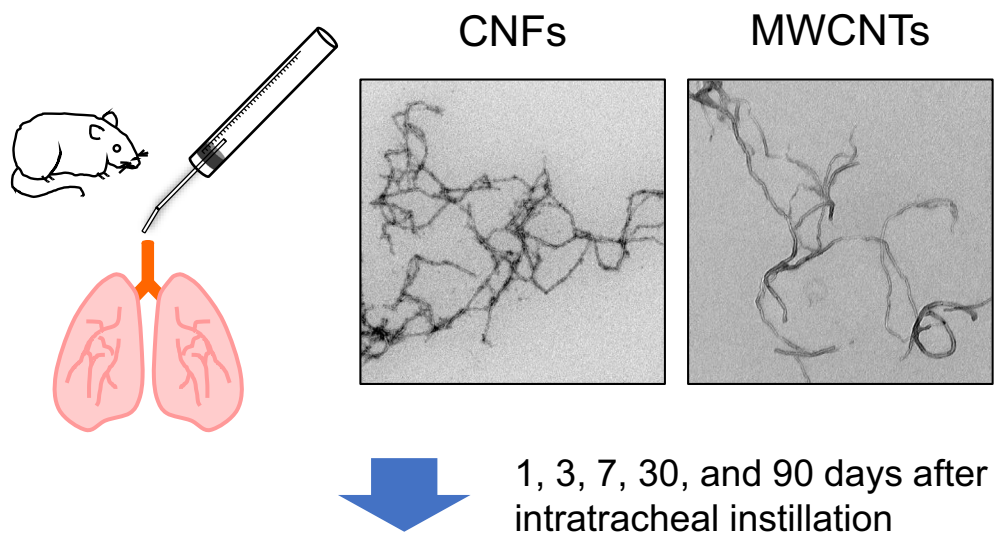
Abstract Safety assessment of cellulose nanofibrils (CNFs) is required to accelerate the utilization of these materials in industrial applications. The present study aimed to characterize the effects on rat pulmonary inflammation over a period of 90 days following intratracheal instillation of three types of CNFs or multi-walled carbon nanotubes (MWCNTs) at doses of 0.5, 1.0, or 2.0 mg/kg. The pulmonary inflammatory responses induced by phosphorylated CNFs (CNF1), 2,2,6,6-tetramethylpiperidine-1-oxyl radical (TEMPO)-oxidized CNFs (CNF2), CNFs produced via mechanical defibrillation (CNF3), and MWCNTs were investigated using bronchoalveolar lavage fluid analysis, histopathological findings, and comprehensive gene expression profiling of rat lungs. CNF1 and CNF2 with approximately equal diameter (7.0–8.0 nm) and length (0.8–1.0 μm) distributions induced inflammation after dosing, which was attenuated 90 days post-instillation. CNF3 of relatively

greater thickness (21.2 nm) and longer length (1.7 μm) deposited around the terminal bronchioles were observed after instillation. Acute inflammatory responses in the alveoli induced by CNF3 were mild compared with those induced by other materials and attenuated 90 days post-instillation. MWCNTs induced severe pulmonary inflammatory responses that continued during the test period. The inflammation failed to resolve within 90 days post-instillation. A hierarchical cluster analysis revealed comparable gene expression profiles for CNF1, CNF2, and CNF3, whereas profiles of MWCNTs were different from those of other test substances. This study suggests that pulmonary inflammation is associated with the diameter and length distributions of CNFs and that the pulmonary inflammation caused by CNFs is mild compared with that caused by MWCNTs.

Supplementary Information The online version contains supplementary material available at <https://doi.org/10.1007/s10570-021-03943-2>.

K. Fujita (✉) · S. Obara · J. Maru · S. Endoh
Research Institute of Science for Safety and Sustainability (RISS), National Institute of Advanced Industrial Science and Technology (AIST), Tsukuba, Ibaraki 305-8569, Japan
e-mail: ka-fujita@aist.go.jp

Graphic abstract



Pulmonary inflammation

- Cells, total protein, LDH and cytokines in BALF
- Histopathological examination
- Comprehensive gene expression analysis

Keywords Cellulose nanofibrils · Multi-walled carbon nanotubes · Intratracheal instillation · Pulmonary inflammation

Introduction

Cellulose nanofibrils (CNFs), also known as cellulose nanofibers or nanofibrillated cellulose (NFC), are light, strong, and have low thermal expansion. Industrial products are being developed in various fields on a global scale (Kangas 2013; Sharma et al. 2019; Trache et al. 2020). These materials are characterized as cellulose nanosized objects, with an aspect ratio of typically > 10 , and may exhibit longitudinal divisions, entanglements between particles, or network-like structures. The dimensions are typically 3–100 nm in diameter and up to 100 μm in length (ISO/TS 20477: 2017).

However, toxicity of CNFs is noted because the material possesses unique physicochemical properties, including fibrous and ultrafine size not displayed

by existing chemicals (Shatkin and Kim 2015). The potential safety concern is the exposure of workers to CNFs in the work environment and use by consumers, such as through spray products. To promote safe commercialization, it is necessary to ensure safety during handling (Shatkin et al. 2016). Assessments on occupational exposure to CNFs in manufacturing facilities have been reported to enhance the understanding and management of the risk of inhaling dried nanocellulose powders during their handling in the workplace (Ogura et al. 2020). Exposure in such situations usually involves inhalation or dermal contact and primary target organs will be lung and skin. Toxicological assessment is required for both pulmonary and dermal effects.

Inhalation exposure and intratracheal instillation using rodents, such as rats and mice, are reported for evaluating pulmonary toxicity of nanomaterials (Silva et al. 2014; Morimoto et al. 2012). Intratracheal instillation involves single or multiple doses administered directly into the trachea of rodents, with follow-up observation. Such tests are simpler and use smaller amounts of test material in comparison

with inhalation exposure test. Moreover, dose to the lungs can be determined precisely, and intratracheal instillation has been used for evaluating the toxicity of several nanomaterials (Kobayashi et al. 2019; Fujita et al. 2016; Honda et al. 2017). We believe that the intratracheal instillation using test material dispersed in liquid is appropriate for evaluating CNF dispersed in an aqueous solvent. Pulmonary exposure to 6 or 18 μg of NFC administered by intratracheal instillation induced pulmonary inflammation, genotoxicity, and systemic acute phase response 28 days post-exposure (Hadrup et al. 2019). However, to the best of our knowledge, no reports of intratracheal instillation of CNFs with long-term follow-up are available (Sai and Fujita 2020; Ventura et al. 2020).

CNFs have properties intermediate between gel and sol, and viscosity changes with time and shear stress (i.e., thixotropy) (Nechyporchuk et al. 2016a). Furthermore, the physicochemical properties of CNFs, such as fiber diameter, fiber length, morphology, functional groups, and impurities, vary depending on raw materials and chemical–mechanical treatment (Nechyporchuk et al. 2016b; Isogai et al. 2011; Isogai 2013). The safety of different grades of fibrillated celluloses should be assessed case by case (Pitkänen et al. 2014). In this study, we selected two types of CNFs produced via chemical modification, phosphorylated CNFs and 2,2,6,6-tetramethylpiperidine-1-oxyl radical (TEMPO)-oxidized CNFs, and one produced via mechanical defibrillation of needle bleached kraft pulp. Moreover, one type of multi-walled carbon nanotubes (MWCNTs) was selected as a reference material. CNF or MWCNT suspensions were prepared and their physicochemical properties were characterized, after which they were used for rat intratracheal instillation test at three doses (0.5, 1.0, and 2.0 mg/kg). Morphological observations, bronchoalveolar lavage fluid (BALF) analysis, histopathological examination, and comprehensive gene expression profiles were examined up to 90 days after instillation to assess pulmonary inflammation.

Materials and methods

Test materials

Aqueous slurries of 20 mg/mL phosphorylated CNFs (hereinafter referred to as “CNF1”), 10 mg/mL

TEMPO-oxidized CNFs (referred to as “CNF2”), and 20 mg/mL CNFs produced via mechanical defibrillation (referred to as “CNF3”) were obtained from Oji Holdings Corporation, Ltd. (Tokyo, Japan), Nippon Paper Industries Co. Ltd. (Tokyo, Japan), and Daio Paper Corporation (Tokyo, Japan), respectively. CNF1 suspensions containing 10 $\mu\text{g}/\text{mL}$ benzalkonium chloride (BAC) and CNF2 suspensions containing preservatives were adjusted to a concentration of approximately 2.0 mg/mL using a planetary centrifugal bubble-free mixer (ARE-310, THINKY CORPORATION, Tokyo, Japan) for 60 min (Sai et al. 2020). CNF3 containing 10 $\mu\text{g}/\text{mL}$ BAC were adjusted to a concentration of approximately 2.0 mg/mL using an ultrasonic mixer (PR-1, THINKY CORPORATION, Tokyo, Japan) for 3 min. Each estimated 2.0 mg/mL aqueous suspension was diluted to a concentration of 0.5, 1.0, and 2.0 mg/mL using each of the preservative solutions and agitated gently for the animal test. The mass of CNFs was determined from the weight loss by evaporation after oven drying at 105 °C for 3 h.

Bulk NC7000TM Nanocyl-MWCNTs were purchased from Nanocyl SA (Chiba, Japan). MWCNTs were dispersed in 10 mg/mL bovine serum albumin (BSA; NACALAI TESQUE, INC., Kyoto, Japan) solution dissolved in UltraPureTM DNase/RNase-Free distilled water (Thermo Fisher Scientific, Waltham, MA, USA) using a Branson 1510 J-DTH ultrasonic bath (Branson Ultrasonics, Emerson Japan, Ltd., Atsugi, Japan). MWCNTs suspension was filtered through a cell strainer with a 40 μm nylon mesh (Nippon Becton Dickinson Company, Ltd., Tokyo, Japan) to remove large carbon nanotube agglomerates. The concentration of MWCNTs in the filtrates was determined by measuring their ultraviolet (UV)-visible absorption spectra using a UV-2550 spectrophotometer (Shimadzu Corporation, Kyoto, Japan) at wavelengths of 600–800 nm (Fujita et al. 2020). The filtrates, hereafter referred to as “MWCNT,” were adjusted at a concentration of 0.5, 1.0, and 2.0 mg/mL in 10 mg/mL BSA solution and used for animal tests.

Physicochemical properties of CNFs and MWCNTs

An H-7100 transmission electron microscopy (TEM) system operating at 100 kV (Hitachi, Ltd., Tokyo, Japan) was used to observe CNFs and MWCNTs.

Uranyl acetate was used for TEM staining of CNFs. The lengths and fiber diameters of CNFs and MWCNTs were measured from approximately 250 or 1000 CNFs and MWCNTs, respectively, using a JEM-1010 TEM (JEOL Ltd., Tokyo, Japan) at 100 kV. The viscosity of aqueous CNF suspensions was measured using an MCR-302 rheometer (Anton Paar, Graz, Austria) over a shear rate range of 0.1–1000 s⁻¹ (*D*) following the manufacturer's protocol. No bacterial or fungal colonies and mycoplasma were detected in three CNF aqueous suspensions using 3 MTM PetrifilmTM (3 M Japan Limited, Tokyo, Japan) and MycoAlertTM Mycoplasma Detection Kit (Lonza, LT07-118 and LT07-518, Tokyo, Japan). A Limulus amoebocyte lysate test (Associates of Cape Cod, Inc., East Falmouth, MA, USA; data not shown) was conducted to find endotoxins in MWCNT suspensions, but none was detected.

Animals

All animal tests were performed at the BioSafety Research Center Inc., Iwata, Japan. The rats were housed in metal cages (W 19.7 × D 26.3 × H 18.0 cm) in a room with 35%–70% humidity (actual value: 39%–74%) and a controlled temperature of 20–26 °C (actual value: 22.6–23.5 °C) and were fed a chow diet (Oriental Yeast Co., Ltd. Tokyo, Japan) ad libitum. After a 1-week acclimation, 720 7-week-old male Crl:CD (Sprague–Dawley) male rats (Charles River Laboratories Japan, Yokohama, Japan) were divided into eight groups including four vehicle control groups, three CNF-administered groups, and one MWCNT-administered group. The body weight before instillation treatment was 227–307 g.

Experimental design

Rats were anesthetized with isoflurane (Viatris Inc., Tokyo, Japan) and intratracheally instilled once with 1.0 mL test solutions (CNF1, CNF2, CNF3, MWCNT, and their vehicle control) per 1 kg body weight using a feeding needle (Natsume Seisakusho Co., Ltd., Tokyo, Japan). The CNF and MWCNT suspensions were lightly shaken before administration to minimize aggregation. We ensured that the tip of the feeding needle was carefully positioned in the trachea near to, but not touching, the carina for appropriate intratracheal instillation. The dose of CNFs or MWCNTs was

determined to be 0.5, 1.0, and 2.0 mg/kg. The reason for selecting the maximum dose of 2.0 mg/kg was that preliminary test observed irregular respiration and death in a few rats after intratracheal instillation of a dose of 5.0 mg/kg CNF1, CNF2, and CNF3 (data not shown).

After instillation, viability and general condition of the rats were recorded once a day until they were sacrificed. Body weight was measured before instillation and at 1, 3, and 7 days post-installation and once a week thereafter. Lung and liver weight were measured at 1, 3, 7, 30, and 90 days post-instillation. Morphological observations, BALF analysis, histopathological examination, and comprehensive gene expression analyses were performed on dissected lungs at 1, 3, 7, 30, and 90 days post-instillation (*n* = 9 per group per time point).

All animal experiments were approved by the Institutional Animal Care and Use Committee of the National Institute of Advanced Industrial Science and Technology, Tsukuba, Japan, and the BioSafety Research Center Inc.

Cell counts, total protein, and proinflammatory cytokine assays with bronchoalveolar lavage fluids

Rats were anesthetized with isoflurane (Viatris Inc.) and euthanized by exsanguination. The left bronchus was clamped with forceps, and the right bronchus was cannulated. Subsequently, 3 mL of warm (37 °C) phosphate-buffered saline (PBS; Thermo Fisher Scientific K.K., Tokyo, Japan) was filled and aspirated to and from the right lungs to recover the BALF. This procedure was repeated three times. Supernatants were obtained by centrifuging BALFs and used for total protein, lactate dehydrogenase (LDH), and cytokine measurements. Centrifuged pellets were suspended in PBS and used for cell counts. The total number of cells in BALFs was counted using a hematology system (ADVIA120, Siemens Healthcare Diagnostics, Inc., Tokyo, Japan). The total number of nucleated cells—neutrophils, macrophages, eosinophils, basophils, and lymphocytes—was counted after May–Grünwald–Giemsa staining. Total protein and LDH in BALFs were measured with an automatic biochemical analyzer (7170, Hitachi High-Tech Fielding Corporation, Tokyo, Japan). The levels of proinflammatory cytokines, including interleukin-1 alpha (IL-1 α), macrophage inflammatory protein-1 alpha

(MIP-1 α), interleukin-1 beta (IL-1 β), macrophage chemoattractant protein-1 (MCP-1), interleukin-18 (IL-18), secreted phosphoprotein 1 (SPP1, also known as osteopontin), gamma interferon (IFN γ), and tumor necrosis factor-alpha (TNF- α), were measured using a MILLIPLEX[®] MAP Rat Cytokine/Chemokine Magnetic Bead Panel, MILLIPLEX[®] MAP Rat Kidney Toxicity Magnetic Bead Panel 1, and a Luminex 200 System (Merck Ltd., Tokyo, Japan).

Histopathological analysis

After rats were sacrificed, their left lungs were filled with 10% buffered paraformaldehyde before processing for histopathological examinations. Fixed left lung tissues were embedded in paraffin and stained with hematoxylin and eosin. Digital images of each lung section were obtained for the alveoli, alveolar walls, bronchioles, and vessels for histopathological evaluation.

RNA extraction and DNA microarray experiments

Right lungs ($n = 4$ per group per time point) were homogenized using the QIAzol Lysis Reagent and a TissueRuptor (QIAGEN K.K., Tokyo, Japan). Total RNA from homogenates was extracted using the RNeasy Midi Kit (Qiagen), following the manufacturer's instructions. RNA was quantified using a NanoDrop 2000 spectrophotometer (Thermo Fisher Scientific), and sample quality was monitored with an Agilent 2100 Bioanalyzer (Agilent Technologies, Santa Clara, CA, USA). Cyanine-3-labeled complementary RNA (cRNA) was prepared from RNA using a Low Input Quick Amp Labeling kit (Agilent Technologies) following the manufacturer's instructions and purified on the RNeasy column (QIAGEN K.K.). Each labeled cRNA probe was used separately for hybridization to a 4×44 K G2519F#14879 Whole Rat Genome Microarray (Agilent Technologies) for 17 h at 65 °C. Hybridized microarray slides were washed following the manufacturer's instructions and scanned using a G2565BA DNA Microarray Scanner (Agilent Technologies) at a resolution of 5 μ m. Finally, scanned images were analyzed numerically using Agilent Feature Extraction ver. 12.0.3.1 (Agilent Technologies).

Microarray data analysis

Normalized data were analyzed using GeneSpring GX ver. 14.9 (Agilent Technologies). Log-fold-changes (FCs) represent the ratio of normalized intensity of CNF- or MWCNT-exposed samples to normalized intensity of vehicle control samples. Genes with log FC values > 1 were considered upregulated, whereas those with log FC values < -1 were considered downregulated. A heat map of the expression profile of genes in rats instilled with 2.0 mg/mL of CNFs or MWCNTs was constructed by hierarchical clustering (18,101 probes). Low-quality probes and genes with significant no change in expression ($-1 < \log FC < 1$) were removed from all genes (41,105 probes). This study focused on differentially expressed genes involved in inflammatory responses, responses related to oxidative stress and apoptosis, and extracellular matrix (ECM) degradation. Gene expression profiles for each experimental group were uploaded to the Gene Expression Omnibus database (accession no. GSE154013; <http://www.ncbi.nlm.nih.gov/projects/geo/>).

Statistical analysis

Numerical values are represented as the mean \pm standard deviation (SD). The quantitative values obtained with cell test and biochemical test values in BALF, body weight gain, and organ weights were analyzed by F-test for equality of variances ($p < 0.05$). Student's *t*-test for equal variance and Welch's *t*-test for unequal variance was performed, respectively. *p*-values of < 0.05 were considered statistically significant.

Results

Characterization of CNFs

TEM images of CNF1, CNF2, and CNF3 suspensions showed network structure of dispersed CNFs (Fig. 1). The geometric mean for fiber diameters and lengths were similar for CNF1 and CNF2 suspensions, approximately 7.0–8.0 nm and 0.8–1.0 μ m, respectively (Table 1). Fibers in the CNF3 suspension were comparatively dispersed with greater thickness and longer lengths, 21.2 nm and 1.7 μ m, respectively.

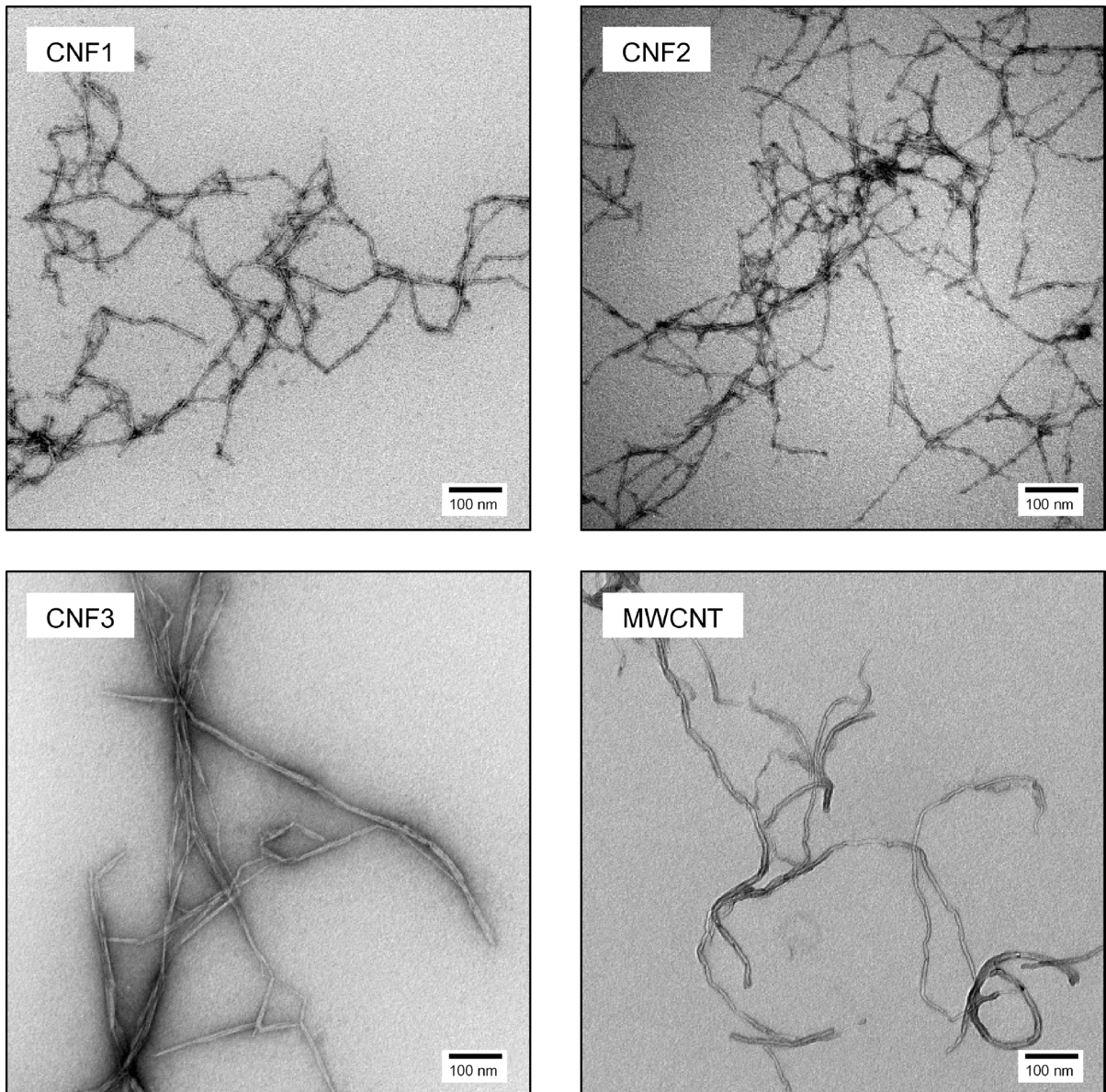


Fig. 1 TEM images of CNF1, CNF2, CNF3, and MWCNT suspensions. TEM, transmission electron microscopy; CNF, cellulose nanofibril; MWCNT, multi-walled carbon nanotube

MWCNT suspensions showed individually dispersed bent CNT fibers. The geometric mean diameter of MWCNTs was similar to that of CNF1 and CNF2, 7.7 nm. MWCNTs were dispersed with a somewhat shorter length, 0.5 μm . No noticeably aggregated CNFs and CNTs were observed in all preparations (data not shown).

CNF1 and CNF2 exhibited pseudoplastic flow behavior at $D > 1$, except at the low shear rate region

(Supplementary Fig. S1, A1 and B1), and curves could be described with the equation of pseudoplasticity $\tau = kD^n$.

$$\text{CNF1} \quad k : 0.010, n : 0.83$$

$$\text{CNF2} \quad k : 0.025, n : 0.72$$

Apparent viscosity ($\eta = \tau/D$) suggested low shear rate dependence (Supplementary Fig. S1, A2 and B2). CNF2 displayed higher viscosity than CNF1. The flow

Table 1 Characteristics of cellulose nanofibrils and multi-walled carbon nanotubes in suspensions

	Diameter		Length	
	Geometric mean (nm)	Geometric standard deviation	Geometric mean (μm)	Geometric standard deviation
CNF1	7.9	1.6	0.8	1.9
CNF2	7.6	1.5	1.0	1.9
CNF3	21.2	2.0	1.7	2.0
MWCNT	7.7	1.6	0.5	2.3

curve of CNF3 showed decreased τ at $D < 10$, remained nearly constant at $D < 500$, and increased slightly at $D > 500$. The viscosity was almost inversely proportional to D (Supplementary Fig. S1, C1 and C2). These CNF3 properties were distinctly different from CNF1 and CNF2.

General condition of rats

Rats instilled with CNF1 and CNF2 exhibited no abnormalities in general conditions in comparison with vehicle control rats. Respiratory irregularities were observed on the day of instillation (Day 0, 1 to 4 h after instillation) in eight of 45 rats administered 2.0 mg/mL CNF3 but all rats recovered by the next day. No abnormalities in general condition were observed in the rats administered CNF3 of 0.5 and 1.0 mg/mL. Respiratory irregularities were observed on day 0 in one rat that was administered 2.0 mg/mL MWCNTs, but this rat recovered by the next day. No abnormalities in general condition were observed in the rats administered 0.5 and 1.0 mg/mL MWCNTs.

Body weight gain and organ weights

Body weight gain of rats treated with 2.0 mg/kg CNF1 group for days 1 to 21 post-instillations was significantly less in comparison with control rats (Table 2). Body weight gain was also less for rats treated with 1.0 and 2.0 mg/kg CNF2 on days 1–7 and 3, respectively. Body weight gain was significantly less in rats administered 0.5, 1.0, and 2.0 mg/kg CNF3 on days 1, 1–3, and 1–7 post-instillation, respectively. Significant weight gains were observed on days 28 and 30 for rats administered 1.0 mg/kg CNF3 and day 30 for rats receiving 2.0 mg/kg. However, weight gain in control rats remained low during this period, and we conclude that body weight was not affected by

instilled CNF3. Body weight gain was significantly less in rats administered 2.0 mg/kg MWCNTs on day 1 post-instillation. Significantly low weight gains were observed on day 30 post-instillation in rats receiving 1.0 mg/kg MWCNTs. This change was not dose-related, and control rat weight gain remained high during this period, and we conclude that instilled MWCNTs were not the cause of these differences.

Lung weight was significantly greater in rats treated with 2.0 mg/kg CNF1 or CNF3 on days 1–30 post-instillation in comparison with controls (Supplementary Table S1). Lung weight was also significantly greater in rats administered 2.0 mg/kg CNF2 on days 1–7. Lung weight was significantly greater in rats treated with 2.0 mg/kg MWCNTs on days 1–90.

Liver weight was significantly less in rats treated with 1.0 mg/kg and 2.0 mg/kg CNF1 or CNF3 on day 1 post-instillation (Supplementary Table S2). Further, liver weight was significantly less in rats administered 0.5 and 2.0 mg/kg MWCNTs on days 1 and 7.

Cells in BALF

Numbers of total nucleated cells and macrophages in all rats treated with CNF1 increased up to day 7 post-instillation in a dose-dependent manner (Fig. 2). High counts of neutrophils were observed on days 1 post-instillation. Additionally, numbers of eosinophils were significantly elevated up to day 7 in a dose-dependent manner. The total nucleated cells and macrophage counts in all CNF2-treated rats increased up to day 7 post-instillation. High counts of neutrophils and eosinophils were observed on days 1, 3, and 7.

No markedly elevated values in all CNF3-treated rats were observed for the total nucleated cells and macrophages up to day 90 post-instillation. High counts in 1.0 mg/kg and 2.0 mg/kg MWCNT-treated rats were observed for total nucleated cells,

Table 2 Body weight gain of rats after intratracheal instillation of CNFs or MWCNTs: vehicle control rats and animals treated with 0.5, 1.0, and 2.0 mg/kg CNF or MWCNT

Days post instillation		0	1	3	7	14	21	28	30	35	42
Number of rats		45	45	36	27	18	18	18	9	9	9
CNF1	Vehicle	0	4 ± 3	19 ± 5	47 ± 8	88 ± 14	126 ± 19	159 ± 20	168 ± 20	184 ± 22	209 ± 23
	0.5	0	4 ± 3	21 ± 6	48 ± 10	86 ± 17	123 ± 26	157 ± 29	165 ± 23	188 ± 41	219 ± 43
	1.0	0	3 ± 4	17 ± 6	45 ± 9	87 ± 19	125 ± 23	160 ± 26	180 ± 25	175 ± 30	199 ± 32
	2.0	0	-1 ± 7 ^{##}	9 ± 13 ^{##}	35 ± 11 ^{**}	73 ± 11 ^{**}	114 ± 16 [*]	148 ± 22	159 ± 28	175 ± 22	204 ± 29
CNF2	Vehicle	0	5 ± 3	20 ± 5	47 ± 9	84 ± 16	121 ± 21	151 ± 23	170 ± 27	168 ± 23	194 ± 25
	0.5	0	4 ± 4	19 ± 6	46 ± 12	85 ± 21	125 ± 25	161 ± 26	189 ± 23	171 ± 25	198 ± 31
	1.0	0	4 ± 4 [*]	17 ± 5 [*]	42 ± 9 [*]	82 ± 16	119 ± 23	152 ± 26	171 ± 13	165 ± 39	188 ± 44
	2.0	0	1 ± 5 ^{##}	16 ± 6 ^{**}	43 ± 11	79 ± 14	117 ± 19	150 ± 21	157 ± 19	183 ± 30	212 ± 34
CNF3	Vehicle	0	3 ± 3	17 ± 5	42 ± 8	78 ± 19	111 ± 25	142 ± 27	153 ± 33	166 ± 24	190 ± 24
	0.5	0	1 ± 5 [#]	15 ± 6	41 ± 8	80 ± 13	115 ± 18	149 ± 22	162 ± 29	171 ± 20	194 ± 23
	1.0	0	-3 ± 5 ^{##}	13 ± 6 [*]	43 ± 8	85 ± 15	122 ± 22	161 ± 27 [*]	184 ± 27 [*]	172 ± 27	196 ± 26
	2.0	0	-10 ± 7 ^{##}	8 ± 6 ^{**}	37 ± 10 [*]	79 ± 19	116 ± 27	151 ± 33	183 ± 22 [*]	145 ± 37	168 ± 38
MWCNT	Vehicle	0	3 ± 4	17 ± 5	44 ± 8	87 ± 16	125 ± 22	159 ± 24	180 ± 24	173 ± 26	197 ± 30
	0.5	0	2 ± 4	18 ± 5	46 ± 9	90 ± 17	128 ± 24	163 ± 29	185 ± 35	174 ± 28	198 ± 31
	1.0	0	1 ± 5	17 ± 7	45 ± 13	83 ± 25	120 ± 35	154 ± 43	157 ± 21 [*]	187 ± 61	212 ± 67
	2.0	0	-2 ± 6 ^{##}	16 ± 6	48 ± 10	87 ± 13	125 ± 18	162 ± 23	175 ± 23	182 ± 31	208 ± 33
Days post instillation			49	56	63	70	77	84	90		
Number of rats			9	9	9	9	9	9	9		
CNF1	Vehicle	226 ± 24	244 ± 25	258 ± 27	271 ± 27	282 ± 30	292 ± 32	302 ± 34			
	0.5	241 ± 41	265 ± 43	281 ± 43	299 ± 41	314 ± 45	329 ± 45	341 ± 47			
	1.0	219 ± 31	239 ± 32	253 ± 33	269 ± 33	282 ± 34	293 ± 34	304 ± 36			
CNF2	Vehicle	226 ± 36	249 ± 38	263 ± 40	281 ± 45	295 ± 48	309 ± 54	320 ± 55			
	0.5	219 ± 33	239 ± 33	252 ± 31	266 ± 33	279 ± 34	288 ± 34	299 ± 36			
	1.0	206 ± 47	224 ± 48	234 ± 50	247 ± 53	258 ± 56	270 ± 59	280 ± 60			
CNF3	Vehicle	229 ± 38	251 ± 41	268 ± 45	282 ± 44	297 ± 47	312 ± 51	323 ± 51			
	0.5	214 ± 27	232 ± 28	248 ± 32	263 ± 31	273 ± 34	285 ± 34	296 ± 37			
	1.0	215 ± 27	232 ± 29	249 ± 30	264 ± 31	278 ± 32	286 ± 34	299 ± 35			
2.0	188 ± 39	207 ± 37	222 ± 37	234 ± 37	243 ± 40	253 ± 40	261 ± 41				

Table 2 continued

Days post instillation	49	56	63	70	77	84	90
Number of rats	9	9	9	9	9	9	9
MWCNT							
Vehicle	219 ± 32	238 ± 34	252 ± 39	265 ± 41	277 ± 46	289 ± 45	299 ± 47
0.5	216 ± 36	234 ± 38	249 ± 40	264 ± 43	274 ± 42	283 ± 43	295 ± 48
1.0	232 ± 69	251 ± 72	271 ± 75	287 ± 77	299 ± 77	309 ± 82	322 ± 86
2.0	225 ± 35	243 ± 39	263 ± 44	277 ± 46	287 ± 49	295 ± 51	307 ± 51

Values are mean ± SD (g)

CNF cellulose nanofibril, MWCNT multi-walled carbon nanotube

$p < 0.05$, ## $p < 0.01$, Welch's t -test; * $p < 0.05$, ** $p < 0.01$, Student's t -test vs vehicle control rats

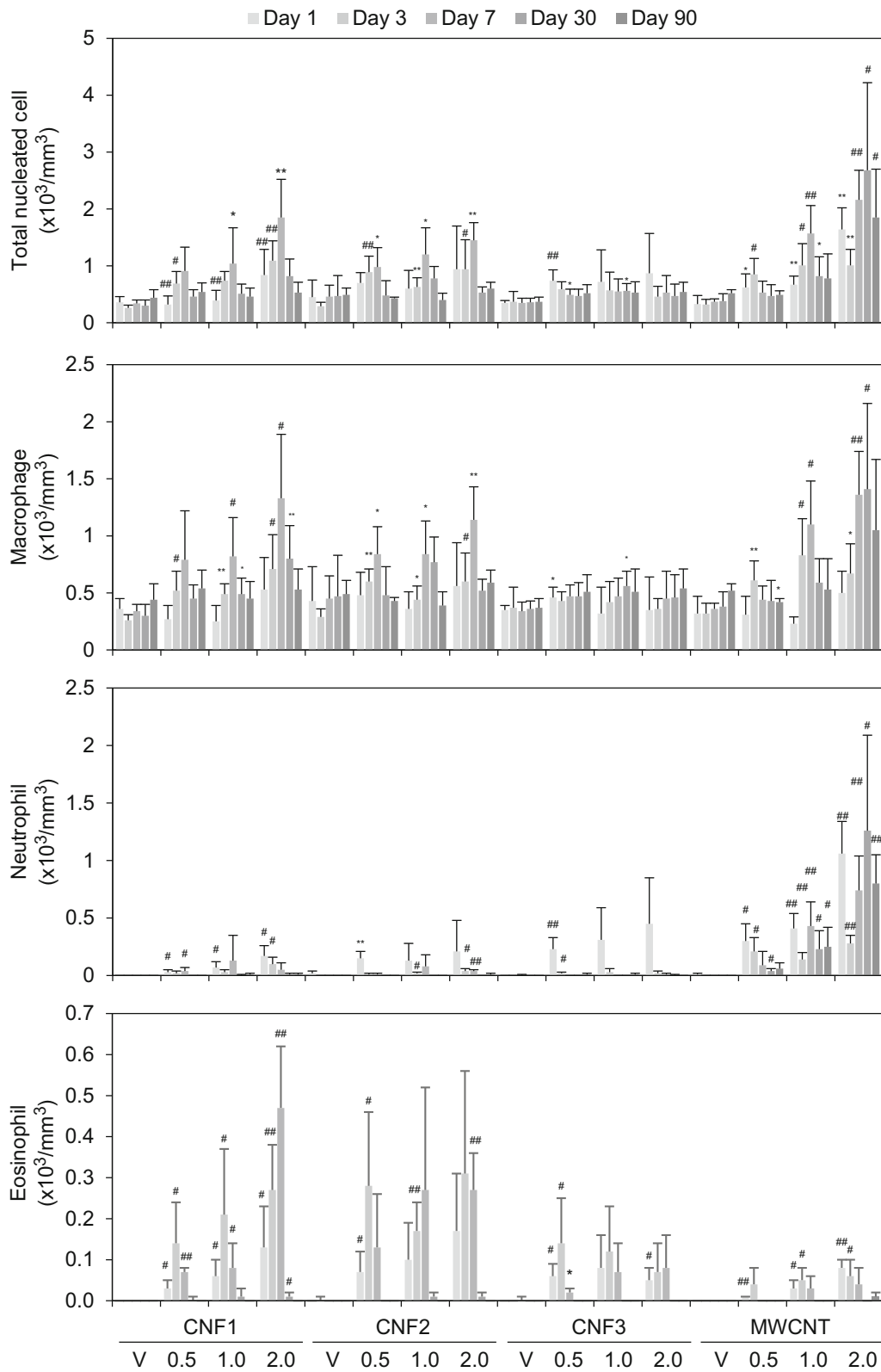
macrophages, and neutrophils on days 1, 3, 7, and 30 post-instillations. These cell numbers were not comparable with those of vehicle control in 2.0 mg/kg MWCNT-treated rats on 90 days post-instillation. Macrophages displaying phagocytic images were observed in MWCNT-treated rats during the observation period. We classified these cells as atypical macrophages and distinguished them from normal nonphagocytosing macrophages. An elevated atypical macrophage to total macrophage ratio was calculated for days 1–90 post-instillations (data not shown). No change was observed in the number of lymphocytes and basophils in all rats treated with CNFs or MWCNTs during the observation period (data not shown).

Total protein and LDH in BALF

High levels of total protein were determined in rats treated with 0.5 and 1.0 mg/kg CNF1 from days 1 to 7, and 2.0 mg/kg CNF1 during the observation period, respectively. LDH in BALF from rats instilled with CNF1 increased from days 1 to 7 post-instillation and recovered to the same level as the control on day 90 (Fig. 3). High levels of total protein and LDH in BALF were determined in rats instilled with CNF2 from days 1 to 7 post-instillation and decreased at days 30 post-instillation. Total protein and LDH levels were elevated in rats instilled with 0.5 and 1.0 mg/kg CNF3 on days 1–3 post-instillation, and 2.0 mg/kg CNF1 on days 1–7 post-instillation. These levels decreased at day 30 post-instillation. Total protein and LDH levels were high in rats treated with MWCNTs during the entire observation period. No recovery was observed in the levels in 2.0 mg/kg MWCNT-treated rats at 90 days post-instillation, compared with those of vehicle control.

Proinflammatory cytokines in BALF

Figure 4 shows the production of IL-1 α , MIP-1 α , IL-1 β , MCP-1, and IL-18, SPP1 in BALF of rats after intratracheal instillation of CNFs or MWCNTs. Amount of IL-1 α was high in the rats administered CNF1 and CNF2 on day 3 post-instillation and in the rats administered 2.0 mg/kg MWCNTs on day 1 post-instillation. MIP-1 α and IL-1 β in rats instilled with CNFs were significantly high on day 1 or 3 post-instillation and decreased over time. The MIP-1 α and



◀ **Fig. 2** Total nucleated cell, neutrophil, macrophage, and eosinophil counts in BALF from the CNF1, CNF2, CNF3, MWCNT, and their vehicle control rats. BALF, bronchoalveolar lavage fluid; CNF, cellulose nanofibril; MWCNT, multi-walled carbon nanotube; V, vehicle control. * $p < 0.05$, ** $p < 0.01$ (vs. vehicle control, Student's *t*-test). # $p < 0.01$, ## $p < 0.05$ (vs. vehicle control, Welch's *t*-test)

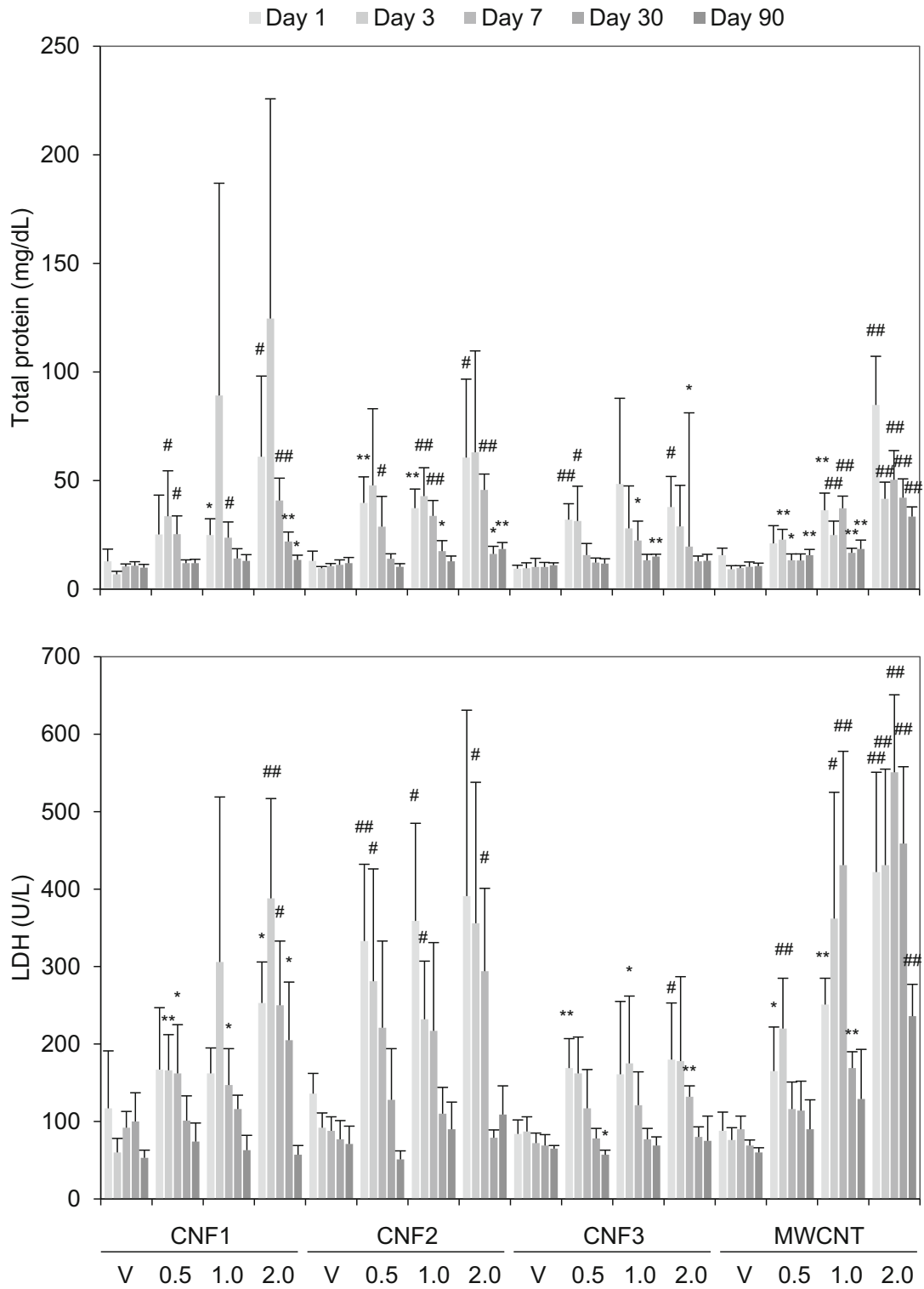
IL-1 β levels in rats instilled with MWCNTs were significantly elevated during the observation period. No recovery was observed in the levels at 90 days post-instillation, compared with those of the vehicle control. MCP-1 was significantly high on days 1 and 3 post-instillation in rats administered 2.0 mg/kg CNFs. No recovery was observed in the levels in 2.0 mg/kg MWCNT-treated rats at 90 days post-instillation. IL-18 was high in rats instilled with MWCNTs on day 1, 3, 7, or 30 post-instillation, respectively. SPP1 in rats instilled with CNFs and MWCNTs was significantly high on days 1 post-instillation and decreased over time. No recovery was observed in the levels in rats instilled with MWCNTs at 90 days post-instillation. No statistically significant differences in the expression of gamma interferon (IFN γ) and tumor necrosis factor-alpha (TNF- α) were observed (data not shown).

Macroscopic findings

Red spots/redness and brown spots/browning of lungs, which is suggesting lung inflammation, were observed in rats instilled with CNFs during the observation period (Fig. 5, A1, A2, B1, B2, C1, and C2). Many cases of browning were observed from days 1 to 7 post-instillation. Black spots/blackening of the lungs was observed in one of nine rats administered with 2.0 mg/mL CNF2 on day 90 post-instillation (Fig. 5, B2d). Black spots in the lung following MWCNTs administration were observed throughout the observation period (Fig. 5, D1 and D2). The black spots on the trachea were observed in five of nine rats instilled with 2.0 mg/mL MWCNTs on day 1 post-instillation (Fig. 5, D1). The black spots/blackening of the pulmonary and parathymic lymph nodes and lymph node swelling was observed in all MWCNT-treated rats from days 7 to 90. The blackening of mediastinal lymph nodes was observed in one case for each MWCNT dose group on day 90 (Fig. 5, D2).

Histopathological examination

Alveolar macrophage numbers increased in CNF1 treated rats, and degeneration/necrosis was also observed. The test substance was deposited in alveoli (Fig. 6, A1) or was observed in macrophages (Fig. 6, A2). Deposition in the alveoli decreased, and uptake by macrophages increased in a time-dependent manner. Inflammatory cell infiltration (intra-alveolar/alveolar wall and blood vessel/peribronchial), bronchial epithelial hyperplasia, and degeneration/necrosis were observed on 1 day post-instillation. Type II alveolar epithelial hyperplasia was observed on day 3 and then subsided in a time-dependent fashion. Numbers and extent were dose-dependent. Furthermore, intra-alveolar hemorrhage was observed in all dose groups. Increased alveolar macrophages and inflammatory cell infiltration (intra-alveolar/alveolar wall and vascular/peribronchial) were observed in a few cases in control rats for the CNF1 group. Alveolar macrophages increased after CNF2 instillation, and test substance deposited as above (Fig. 6, B1 and B2). Granuloma formation was observed 30 days post-instillation (data not shown). Inflammatory cell infiltration (intra-alveolar/alveolar wall and blood vessels/peribronchial), bronchial epithelial hyperplasia, and degeneration/necrosis were observed on day 1, and type II alveolar epithelial hyperplasia was observed on day 3. Both conditions were resolved in a time-dependent manner. Treatment effects were dose-dependent. Intra-alveolar hemorrhage was observed in rats treated with CNF2 and in rats in the control group. Control rats displayed increased alveolar macrophages and infiltration of inflammatory cells (intra-alveolar/alveolar wall, vascular/peribronchial) (data not shown). Alveolar macrophages increased in rats instilled with CNF3, and the test substance CNFs deposited, again as above. Further, deposition around the terminal bronchioles was observed (Fig. 6, C1 and C2). Inflammatory cell infiltration (intra-alveolar/alveolar wall and blood vessels/peribronchial), bronchial epithelial hyperplasia, and degeneration/necrosis were observed on day 1 post-instillation and type II alveolar epithelial hyperplasia was observed on day 3. Findings were again time- and dose-dependent. Intra-alveolar hemorrhage was observed in rats in all dose groups. Inflammatory cell infiltration (intra-alveolar/alveolar wall and blood vessel/peribronchial), bronchial epithelial hyperplasia, and type II alveolar



◀ **Fig. 3** Total protein and LDH in BALF of rats after intratracheal instillation of CNF1, CNF2, CNF3, MWCNT, and vehicle. BALF, bronchoalveolar lavage fluid; LDH, lactate dehydrogenase; CNF, cellulose nanofibril; MWCNT, multi-walled carbon nanotube; V, vehicle control. * $p < 0.05$, ** $p < 0.01$ (vs. vehicle control, Student's *t*-test). # $p < 0.01$, ### $p < 0.05$ (vs. vehicle control, Welch's *t*-test)

hyperplasia were observed in a few cases in control rats (data not shown). Numbers of alveolar macrophages increased in rats after MWCNT instillation, and degeneration/necrosis was observed (Fig. 6, D1 and D2). MWCNTs were deposited in the alveoli or macrophages, and deposition in the alveoli decreased concurrently with an increase in macrophage uptake. Inflammatory cell infiltration (intra-alveolar/alveolar wall and blood vessel/peribronchial), bronchial epithelial hyperplasia, and degeneration/necrosis were observed on day 1 post-instillation; type II alveolar epithelial hyperplasia was observed on day 3 post-instillation. Findings were again time- and dose-dependent. Intra-alveolar hemorrhage was observed in each dose group. The degeneration/necrosis of

alveolar macrophages was observed in the 2.0 mg/mL MWCNT group on day 90 post-instillation. In control rats, inflammatory cell infiltration (vascular/peribronchial) was observed in a few cases.

Comprehensive gene expression analysis

Comprehensive gene expression profiles using a DNA microarray revealed time- and dose-dependent changes in gene expression of rat lungs after intratracheal instillation of CNFs or MWCNTs. Microarray data were deposited in the Gene Expression Omnibus database under Accession Number GSE154013. A hierarchical cluster analysis revealed comparable time-dependent changes in gene expression profiles among 2.0 mg/kg CNF1-, CNF2-, and CNF3-treated rat lungs. However, the profiles of 2.0 mg/kg MWCNTs were different from those of 2.0 mg/kg CNFs (Fig. 7). A large number of upregulated and downregulated genes involved in inflammatory responses and ECM degradation in rat lungs were consistently observed. Fold changes in expression of selected genes are shown in Table 3. *Ccl2*, *Ccl7*,

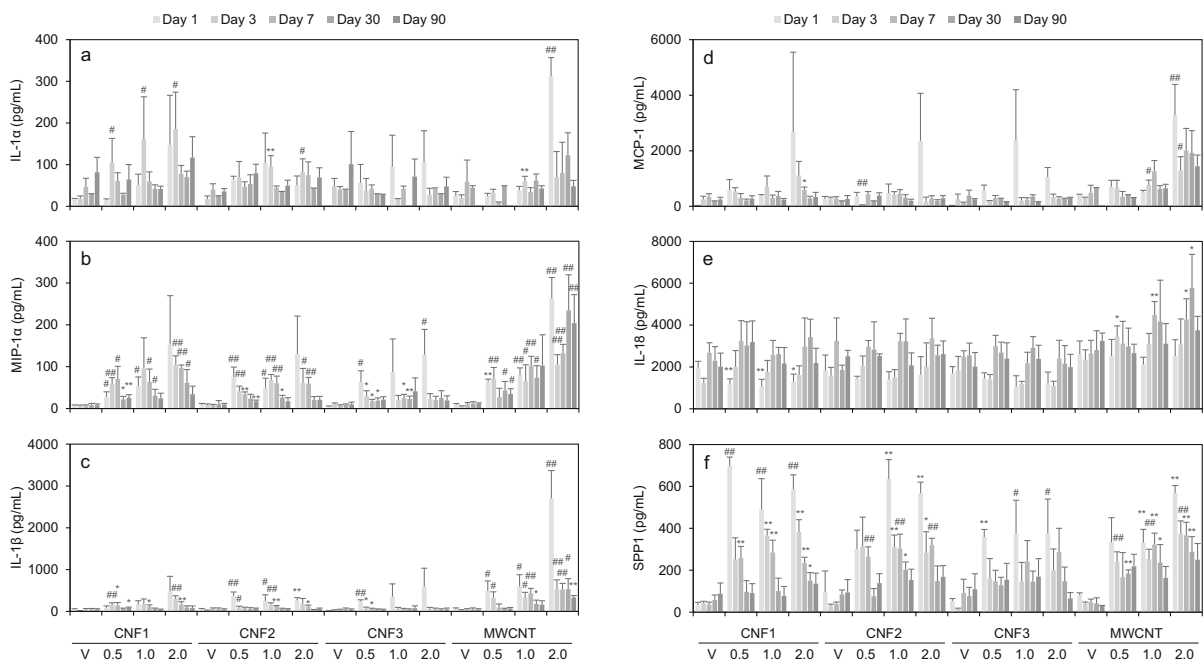
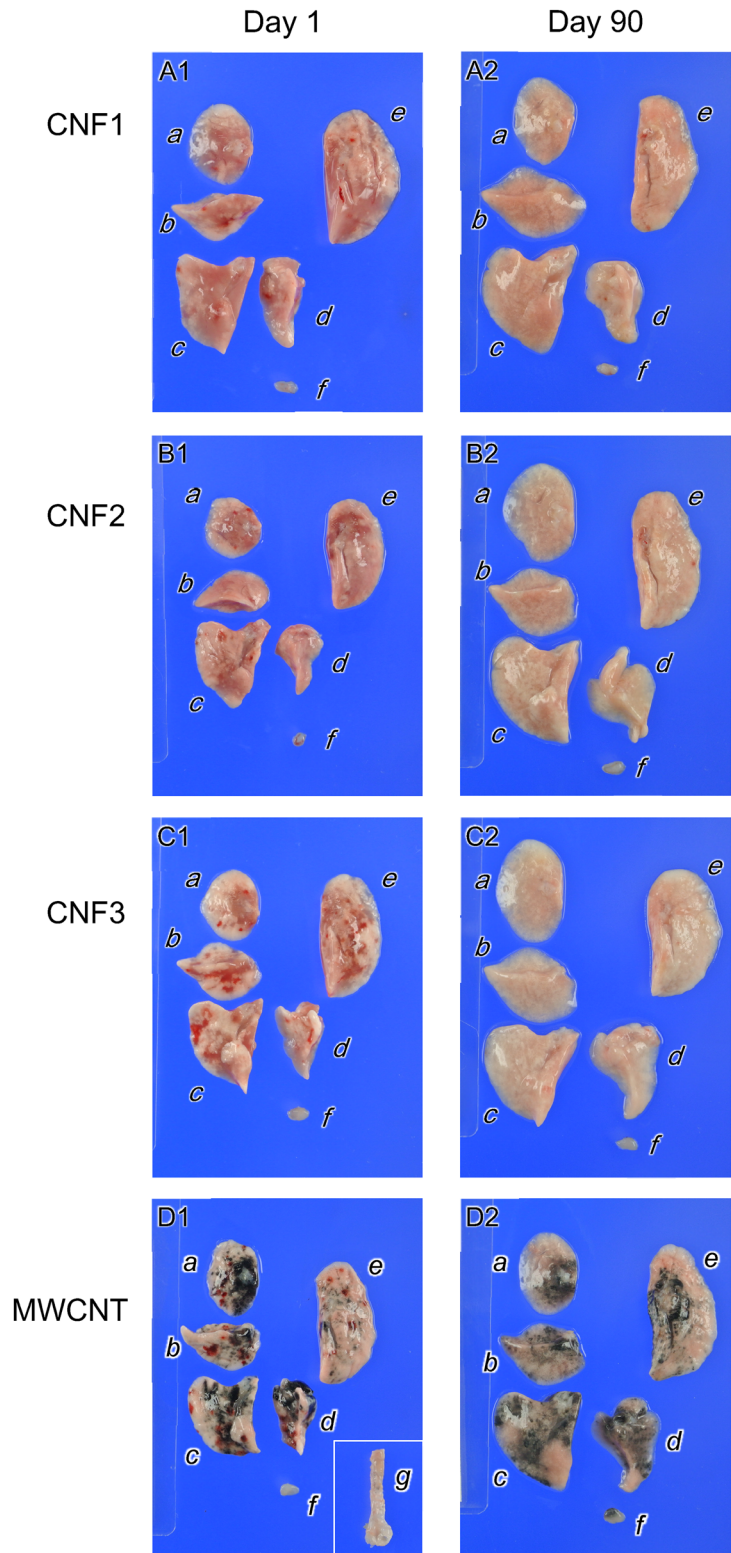
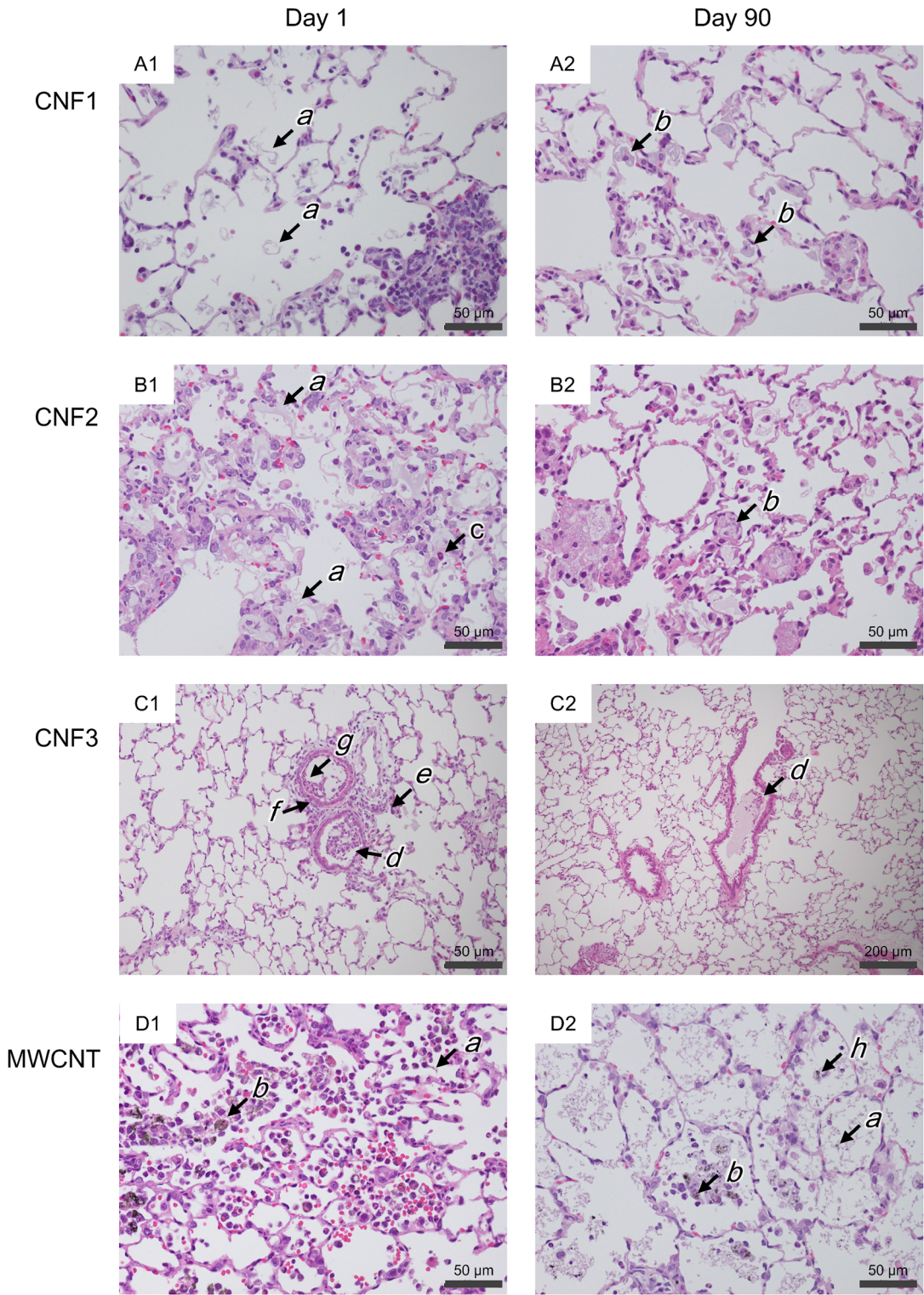


Fig. 4 Proinflammatory cytokines: IL-1 α (a), IL-1 β (c), MCP-1 (d), IL-18 (e), and SPP1 (f) in BALF of rats after intratracheal instillation of CNF1, CNF2, CNF3, MWCNT, and vehicle. BALF, bronchoalveolar lavage fluid; CNF, cellulose nanofibril; MWCNT, multi-walled carbon nanotube; IL-1 α ,

interleukin-1 alpha; MIP-1 α , macrophage inflammatory protein-1 alpha; IL-1 β , interleukin-1 beta; MCP-1, macrophage chemoattractant protein-1; IL-18, interleukin-18; SPP1, secreted phosphoprotein 1; V, vehicle control. * $p < 0.05$ Steel's multiple comparison test vs. vehicle control

Fig. 5 Dissected lungs from rats instilled with 2.0 mg/kg CNF1, CNF2, CNF3, and MWCNT on day 1 and 90 post-instillation. *a*, anterior lobe; *b*, intermediate lobe; *c*, posterior lobe; *d*, accessory lobe; *e*, left lung; *f*, mediastinal lymph nodes; *g*, trachea. CNF, cellulose nanofibril; MWCNT, multi-walled carbon nanotube





◀ **Fig. 6** Histopathology of lung tissues (hematoxylin and eosin staining) of rats instilled with 2.0 mg/kg CNF1 (A1 and A2), CNF2 (B1 and B2), CNF3 (C1 and C2), or MWCNT (D1 and D2) on days 1 day and 90 post-instillation. The lung tissues were fixed in 4% buffered paraformaldehyde, followed by embedding in paraffin. Sections were stained with hematoxylin and eosin. Arrows indicate pathological findings: **a**, Test substance deposition in alveoli; **b**, Test substance in alveolar macrophages; **c**, Inflammatory cell infiltration in the alveoli/alveolar wall; **d**, Test substance deposition in terminal bronchioles; **e**, Peribronchial/perivascular inflammatory cell infiltration; **f**, Bronchial epithelial degeneration/necrosis; **g**, Bronchial epithelial hyperplasia; **h**, Alveolar macrophage degeneration/necrosis

Ccl12, *Ccl17*, *Ccl22*, and *Cxcl2* were highly upregulated after the instillation of CNFs. Gene expression levels decreased levels found in control rats 90 days post-instillation. The genes were also highly upregulated in a dose-dependent manner after the instillation of MWCNTs and continued to be highly expressed even on day 90. *Ccl9* and *Spp1* were remarkably upregulated following all treatments throughout the observation period. *Mmp7*, *Mmp9*, and *Mmp12*, all involved in ECM degradation, were also highly upregulated in CNF-treated rat lungs throughout the observation period. *Mmp7* and *Mmp12* were also highly upregulated following MWCNT administration, but significant upregulation of *Mmp9* was not observed.

Discussion

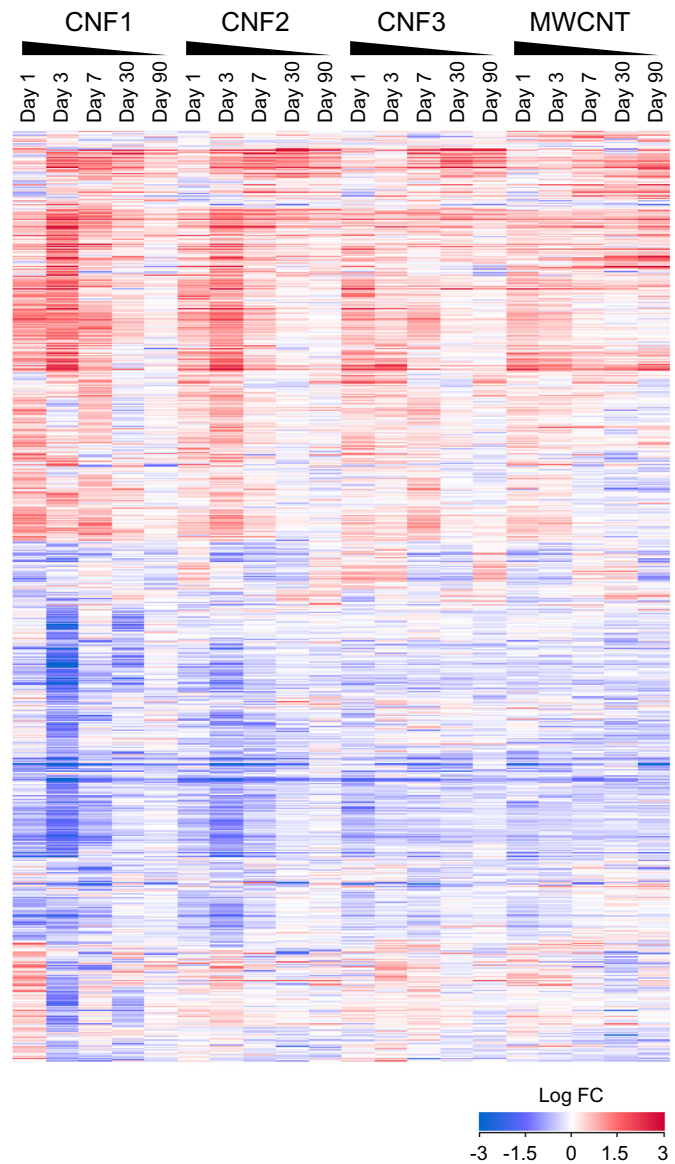
In this study, morphological observations, BALF analysis, histopathological examination, and comprehensive gene expression analysis were examined throughout 90 days after intratracheal instillation of CNFs or MWCNTs. Some reports on animal studies using cellulose nanocrystals (CNCs) are available in the recent literature, although information on animal testing, particularly on subchronic pulmonary toxicity of CNFs, is limited (Endes et al. 2016; Ventura et al. 2020; Sai and Fujita 2020). Pulmonary exposure to CNFs administered to mice by intratracheal instillation induced pulmonary inflammation, genotoxicity, and systemic acute phase response 28 days after exposure (Hadrup et al. 2019). CNFs induced innate immunity responses in vivo 24 h after oropharyngeal aspiration. All effects of CNFs were modest compared with responses induced by rigid MWCNTs (Ilves et al.

2018). CNFs administered by pharyngeal aspiration caused an acute inflammatory response and DNA damage in mouse lung (Catalán et al. 2017). Pulmonary exposure of mice to fibrous materials by oropharyngeal aspiration of crocidolite asbestos led to discrete local immune cell polarization with a TH2-like response and TH1-like immune reaction to NCF. Exposure to CNTs and CNCs caused nonclassical or nonuniform responses (Park et al. 2018). Exposure to respirable CNC via pharyngeal aspiration caused pulmonary inflammation and damage, induced oxidative stress, elevated TGF- β and collagen levels in the lung, and impaired pulmonary function (Shvedova et al. 2016). Pulmonary exposure of mice to CNC by pharyngeal aspiration induced sustained adverse effects in spermatocytes/spermatozoa, suggesting male reproductive toxicity (Farcas et al. 2016). These short-term toxicological assessments, 1–28 days after administration of CNFs or CNCs, may miss effects over longer timeframes and transient and persistent responses cannot be distinguished. We believed that evaluating the effects of medium- to long-term CNF-induced inflammation in this study would be useful for assessing subchronic effects of CNFs.

BALF analysis, histopathological examination, and a comprehensive gene expression analysis confirmed acute inflammation following the instillation of CNFs with different physicochemical properties. Inflammation was attenuated 90 days post-instillation. However, effects differed depending on the characteristics of CNFs. The degree of acute inflammation and attenuation profiles were similar between phosphorylated CNFs and TEMPO-oxidized CNFs. Conversely, CNFs produced via mechanical defibrillation weakly induced acute inflammation. We reasoned that these results reflected the physicochemical properties, particularly the diameter and length distributions of CNFs.

Changes in the expression of several genes associated with inflammatory response and ECM degradation were measured. *Ccl2*, *Ccl7*, *Ccl9*, *Ccl12*, *Ccl17*, *Ccl22*, and *Cxcl2* were highly upregulated by CNF instillation. *Mmp7*, *Mmp9*, *Mmp12*, and *Spp1* were also highly upregulated in the lungs of CNF-treated rats throughout the observation period. Gene expression can be significantly affected by CNFs. However, the regulation of chemokines, MMP, or SPP1 activity is more complex and involves multiple steps, which can complicate the prediction of these activities in

Fig. 7 A heat map generated from comprehensive DNA microarray data reflects differential gene expression patterns in rat lungs instilled with 2.0 mg/mL CNFs or MWCNTs. Genes with low-quality probes and no change in expression ($-1 < \log_{2}FC < 1$) were removed from all genes (41,105 probes) and used (18,101 probes) for a hierarchical cluster analysis. CNF, cellulose nanofibril; MWCNT, multi-walled carbon nanotube



lung tissue. We would like to investigate the enzyme-linked immunosorbent assay or immunohistochemical staining of lung tissues in future studies.

Interestingly, the number of eosinophil in BALF of all CNF1- and CNF2-treated rats were significantly elevated up to day 7 in a dose-dependent manner and recovered after day 30. Eosinophil-rich inflammation has long been associated with parasitic infestation and allergic inflammation (Fulkerson and Rothenberg 2013). Further, numbers of eosinophils in BALF were elevated by house dust mites, jet engine particles, and single-walled carbon nanotubes (Ihrle et al. 2019;

Bendtsen et al. 2019; Inoue et al. 2010). These studies suggest that lung exposure to particles may exacerbate allergic inflammation of the airways. Future research should focus on the association between lung exposure to CNFs and allergic inflammation of the airways.

Phosphorylated CNFs and TEMPO-oxidized CNFs were deposited in the alveoli, whereas CNFs produced via mechanical defibrillation were deposited in the terminal bronchioles following the instillation. Only some latter CNFs reached the alveoli, and the degree of pulmonary inflammation after instillation was thus lower than for phosphorylated CNFs or TEMPO-

Table 3 Fold changes of selected genes involved in inflammatory responses and extracellular matrix (ECM) degradation in rat lungs after intratracheal instillation of 0.5, 1.0, or 2.0 mg/kg CNFs or MWCNTs

Category	Gene name	Genbank	mg/kg	CNF1			CNF2			CNF3			MWCNT			Description								
				1	3	7	30	90	1	3	7	30	90	1	3		7	30	90					
Inflammatory response	<i>Ccl2</i>	NM_031530	0.5	1.7	2.3	0.4	0.1	0.7	2.7	2.0	2.2	0.9	0.5	2.8	1.2	0.1	0.4	1.2	1.7	2.1	1.6	0.7	1.3	Chemokine (C-C motif) ligand 2
			1.0	2.9 ^w	2.2	1.4	0.5	0.5	2.1	2.2	2.9	1.6	0.6	3.5	1.3	1.1	0.9	1.2	2.5	2.3	2.8	1.5	1.8	
			2.0	2.5	3.3	2.3	1.0	0.7	3.9	2.6	3.3	1.9	1.2	3.7	1.3	1.3	1.0	2.4	2.2	2.9	3.3	2.4	3.7	
	<i>Ccl7</i>	NM_001007612	0.5	2.0	2.7	1.1	0.2	0.6	2.8	2.6	2.4	0.7	0.2	2.7	1.3	0.2	0.1	0.7	1.8	2.3	1.9	0.5	1.1	Chemokine (C-C motif) ligand 7
			1.0	3.0	2.2	2.4	0.5	0.0	1.7	2.1	2.6	0.8	-0.3	3.0	1.4	0.8	0.4	0.1	2.5	2.2	2.8	1.4	1.7	
			2.0	2.4	3.9	2.6	1.0	0.6	3.6	2.6	3.1	1.3	0.7	3.4	1.3	0.7	0.2	1.2	2.2	2.8	3.6	2.6	3.8	
<i>Ccl9</i>	NM_001012357	0.5	3.3	2.5	2.9	3.5	1.3	2.5	2.9	3.3	2.6	1.5	2.9	2.1	1.3	3.1	2.8	1.6	1.1	2.1	1.5	1.3	Chemokine (C-C motif) ligand 9	
		1.0	3.2	2.1	4.1	4.2	1.7	2.2	3.5	3.7	3.6	2.2	3.8	2.9	2.7	3.7	2.2	1.2	0.8	2.5	2.5	1.9		
		2.0	2.8	3.7	4.0	3.2	2.3	2.8	3.3	4.0	4.1	3.0	3.2	2.3	2.7	4.3	3.6	0.6	1.0	1.8	2.9	3.4		
<i>Ccl12</i>	NM_001105822	0.5	1.5	2.5	0.7	0.7	0.8	2.3	1.6	2.6	1.1	1.1	2.3	1.8	-0.1	0.1	0.7	1.2	2.2	1.0	0.3	1.4	Chemokine (C-C motif) ligand 12	
		1.0	2.7	3.0	1.9	1.2	0.3	1.0	1.4	2.8	0.8	0.5	2.8	1.5	1.3	0.6	0.4	2.2	2.1	1.9	0.5	1.7		
		2.0	2.1	4.9	1.8	1.8	1.0	3.5	2.2	3.0	1.7	1.3	3.2	1.7	1.3	0.6	0.5	2.3	2.7	2.9	1.7	3.2		
<i>Ccl17</i>	NM_057151	0.5	3.2	3.6	1.3	0.5	0.7	3.1	3.8	1.7	0.9	0.1	3.9	1.9	0.7	1.2	1.0	2.0	2.0	1.3	1.0	0.6	Chemokine (C-C motif) ligand 17	
		1.0	4.6	4.2	2.2	1.1	0.9	2.2	2.9	1.5	0.4	0.2	3.6	2.2	1.3	1.1	0.6	2.3	2.3	1.4	1.2	1.2		
		2.0	3.7	5.1	1.5	1.4	1.0	3.9	4.1	1.6	0.5	0.7	3.8	1.1	1.3	0.8	0.7	1.7	2.3	1.9	1.8	2.5		
<i>Ccl22</i>	NM_057203	0.5	3.6	4.6	1.1	0.5	0.3	3.8	5.2	2.7	0.7	0.6	4.6	2.2	0.8	1.1	1.1	2.3	2.8	2.3	1.4	1.0	Chemokine (C-C motif) ligand 22	
		1.0	5.3	5.8	2.6	1.1	0.3	3.8	4.9	2.4	0.9	0.9	4.7	2.9	1.6	1.4	1.2	3.1	3.4	2.8	1.6	1.7		
		2.0	4.7	6.6	2.2	1.9	0.8	5.4	6.1	2.9	2.0	1.4	4.5	1.3	2.6	1.6	2.6	2.6	3.9	3.2	2.0	3.3		
<i>Cxcl2</i>	NM_053647	0.5	0.5	1.1	0.6	1.4	1.6	1.2	0.6	0.9	0.2	0.8	1.9	0.2	0.2	0.4	1.2	1.6	1.2	1.4	1.1	1.4	Chemokine (C-X-C motif) ligand 2	
		1.0	1.7	0.8	0.5	1.1	1.0	1.5	0.7	1.3	0.3	-0.1	2.7	0.4	0.5	0.6	0.7	1.3	2.1	1.8	2.1	2.3		
		2.0	1.8	1.6	1.2	0.4	0.9	2.6	1.1	0.9	0.0	0.5	3.6	0.8	0.3	0.6	0.8	1.0	1.8	1.8	2.3	3.5		
<i>Spp1</i>	NM_012881	0.5	3.7	4.8	3.0	4.5	2.4	2.6	4.9	4.7	4.3	2.3	2.1	2.6	3.3	5.3	5.3	1.9	3.7	3.3	2.7	2.2	Secreted phosphoprotein 1	
		1.0	3.6	6.3	6.3	6.1	2.8	3.1	5.8	5.4	6.4	4.7	3.8	4.9	5.6	5.9	5.7	2.5	4.0	4.9	4.2	4.0		
		2.0	4.7	7.3	7.8	7.7	4.8	3.1	6.3	6.2	7.4	5.6	3.7	5.4	6.9	7.3	7.1	4.4	6.4	5.6	6.1	6.7		
ECM degradation	<i>Mmp7</i>	NM_012864	0.5	5.1	5.9	4.1	2.3	1.5	4.9	7.1	6.5	3.0	2.1	5.2	4.5	3.3	3.6	3.7	3.9	2.6	2.1	0.6	2.8	Matrix metalloproteinase 7
			1.0	6.8	7.5	7.6	4.3	1.9	3.3	6.2	6.2	4.8	2.8	5.0	5.8	5.1	4.2	4.8	4.3	3.5	2.4	1.2	2.6	

Table 3 continued

Category	Gene name	Genbank	mg/kg	CNF1			CNF2			CNF3			MWCNT			Description								
				1	3	7	30	90	1	3	7	30	90	1	3		7	30	90					
	<i>Mmp9</i>	NM_031055	2.0	5.3	8.7	7.4	5.6	2.4	5.0	8.1	7.7	6.2	3.8	4.9	3.6	5.9	4.9	5.0	3.4	4.6	3.6	2.6	5.8	Matrix metalloproteinase 9
			0.5	1.2	1.6	0.5	0.0	0.3	1.4	2.1	1.2	0.3	0.6	2.4	1.9	1.1	3.2	2.7	1.4	0.5	-0.2	0.4	0.6	
	<i>Mmp12</i>	NM_053963	1.0	2.5	3.5	3.0	1.0	0.3	1.0	2.1	0.9	0.3	0.7	2.9	2.6	1.9	3.8	3.4	0.8	0.6	0.2	0.4	0.6	Matrix metalloproteinase 12
			2.0	2.2	5.9	2.9	1.5	1.1	3.3	4.2	2.4	2.6	1.5	3.4	1.1	2.8	4.7	4.0	0.6	0.4	-0.1	0.6	1.2	
			0.5	3.2	4.6	4.6	3.6	2.2	3.3	4.8	5.6	3.7	2.5	3.6	3.8	2.7	6.0	5.6	2.0	3.2	2.5	2.3	2.1	
			1.0	4.3	5.8	7.3	5.9	4.0	2.7	5.1	6.1	5.7	4.9	4.0	5.4	5.5	7.0	6.4	3.0	4.1	3.8	3.8	3.5	
			2.0	3.7	7.3	8.0	6.8	4.6	4.0	6.0	7.4	7.3	6.2	3.8	3.8	6.4	7.9	7.8	2.5	4.7	4.0	5.5	6.2	

Numerical values represent log-fold gene expression changes relative to negative control levels. Log-fold changes with *p* values < 0.05 are shown in bold CNF cellulose nanofibril, MWCNT multi-walled carbon nanotube

oxidized CNFs. The subsequent behavior of CNFs deposited in alveoli or terminal bronchioles is still unknown. We provided evidence that macrophages phagocytize CNFs as foreign bodies. Some CNFs may have cleared from the lungs, and some may have accumulated. It has been reported that CNTs administered to the lungs may pass through the pleura and translocate through lymphatic drainage in the thoracic cavity to the mediastinal lymph nodes (Murphy et al. 2011). In addition, we have observed using TEM that SWCNTs and MWCNTs are localized in the mediastinal lymph nodes following intratracheal instillation (Fujita et al. 2015, 2016; Honda et al. 2017). This study demonstrated that the blackening of mediastinal lymph nodes was observed in one case for each MWCNT dose group on day 90. On the other hand, it is difficult to distinguish CNFs from lung tissue for gross observation or quantitative analysis because CNFs are a biological substance and have light transmission properties. A novel method is needed for specific and sensitive detection of CNFs in biological tissue. As an example, a simple and robust method using a biotinylated carbohydrate binding module of β-1,4-glycanase from the bacterium, *Cel-lulomonas fimi*, has been developed (Knudsen et al. 2015). Methods for determining CNF clearance from lung tissue will be the subject of future research.

Our results demonstrate that acute inflammation induced by MWCNTs was not attenuated by day 90 post-instillation, in contrast to attenuation of inflammation following CNF instillation. Several studies on the pulmonary toxicity of MWCNTs using in vivo rodent models are available (Kasai et al. 2016; Morimoto et al. 2012; Pauluhn 2010; Muller et al. 2005; Fujita et al. 2016). A 90-day inhalation toxicity study was performed with the same Nanocyl NC7000™ MWCNT material used in this study. Increasing lung weights, pronounced multifocal granulomatous inflammation, diffuse histiocytic and neutrophilic inflammation, and intra-alveolar lipoproteinosis were observed in lung and lung-associated lymph nodes following exposure to 0.5 and 2.5 mg/m³ (Ma-Hock et al. 2009). Furthermore, neutrophil infiltration and CNT uptake into macrophages were observed, consistent with the results of this study. TEM observation showed that entangled Nanocyl NC7000™ MWCNT fibers were found in the cytoplasm within membrane-bound structures (presumably phagosomes) of alveolar macrophages

(Treumann et al. 2013). Our latest in vitro cell-based assays demonstrate that numerous bent MWCNT aggregates were phagocytosed into vacuole-like compartments of NR8383 cells exposed to Nanocyl NC7000TM MWCNT. The results differed from the results using rigid and needle-shaped MWCNTs observed in the cytoplasm in NR8383 cells exposed (Fujita et al. 2020). These in vivo and in vitro assays suggest that Nanocyl NC7000TM MWCNTs are phagocytosed, as are phosphorylated CNFs or TEMPO-oxidized CNFs. Further, both fiber diameter and length (i.e., aspect ratio) of MWCNTs in the suspensions used in this study was similar to dimensions of phosphorylated CNFs or TEMPO-oxidized CNFs. Nevertheless, the effects of CNFs on pulmonary inflammation were modest compared with those of MWCNTs. One explanation for continuing the acute inflammation induced by Nanocyl NC7000TM MWCNT might be an insufficient clearance of MWCNTs instilled into the lung. Conversely, acute inflammatory responses to CNFs might be attenuated by degradability or metabolism in the lungs. The role of biopersistence in fiber effects is well understood and has a profound effect on the clearance and toxicity of fibers (Donaldson et al. 2013). Elucidation of the mechanism of CNF persistence is an issue for future research.

Occupational exposure limits (OELs) are widely recognized as valuable tools for managing worker exposure to chemicals and other hazards in the workplace (Gordon et al. 2014). The Lowest Observed Adverse Effect Level (LOAEL) obtained in a 90-day inhalation exposure study of rats with granulomatous inflammation of the lung as the endpoint using Nanocyl NC7000 was 0.1 mg/m³ (Ma-Hock et al. 2009). The Safety Data Sheet of NC7000TM indicates that no official OELs have been established yet; however, DNEL (Derived No Effect Level) is 0.05 mg/m³ for long-term exposure of MWCNTs (<https://www.nanocyl.com/wp-content/uploads/2020/05/DM-M-3b-1-0-1-SDS-NC3100-V11.pdf>). Since no inhalation exposure test for CNFs has been performed, the LOAEL of CNFs cannot be calculated. In addition, a limitation of this study is that it relies on assessing the inflammatory response as an endpoint to examine pulmonary toxicity following intratracheal instillation of CNFs. If endpoints other than the inflammatory response, such as immune response or carcinogenicity, are found, they need to be revisited.

However, considering the results of inflammation and attenuation of CNFs used in this study, it is most likely that the LOAEL of CNFs may be equal to or higher than those of Nanocyl NC7000. This study will help in establishing occupational exposure levels to manage the risks of CNFs in the workplace.

Conclusion

This study demonstrated rat pulmonary inflammatory responses following intratracheal instillation of CNFs with different physicochemical properties. Acute inflammation following exposure to CNFs decreased over time. Differences in pulmonary inflammatory responses among CNFs were associated CNF shape and size distributions by the CNF manufacturing processes. We suggest that the pulmonary toxicity of CNFs should be assessed depending on the different physicochemical properties of CNFs, such as diameter, length, morphology, functional groups, and impurities. Furthermore, the degree of pulmonary inflammation induced by CNFs was low compared with that induced by MWCNTs, which persisted throughout the study period following exposure. The findings of this study will be informative for establishing the occupational exposure levels of various CNFs, which differ depending on the manufacturing processes or physicochemical properties.

Acknowledgments This study was supported by Project Grants (JPNP13006 and JPNP20009) from the New Energy and Industrial Technology Development Organization (NEDO). The authors thank Dr. Hideo Kajihara (AIST, Japan) for the valuable contribution to the discussion of the results of this study.

Declarations

Conflict of interest The authors declare that they have no competing interests.

Open Access This article is licensed under a Creative Commons Attribution 4.0 International License, which permits use, sharing, adaptation, distribution and reproduction in any medium or format, as long as you give appropriate credit to the original author(s) and the source, provide a link to the Creative Commons licence, and indicate if changes were made. The images or other third party material in this article are included in the article's Creative Commons licence, unless indicated otherwise in a credit line to the material. If material is not included in the article's Creative Commons licence and your intended use is not permitted by statutory regulation or exceeds

the permitted use, you will need to obtain permission directly from the copyright holder. To view a copy of this licence, visit <http://creativecommons.org/licenses/by/4.0/>.

References

- Bendtse KM, Broström A, Koivisto AJ, Koponen I, Berthing T, Bertram N, Kling KI, Dal Maso M, Kangasniemi O, Poikkimäki M, Loeschner K, Clausen PA, Wolff H, Jensen KA, Saber AT, Vogel U (2019) Airport emission particles: exposure characterization and toxicity following intratracheal instillation in mice. *Part Fibre Toxicol* 16:23. <https://doi.org/10.1186/s12989-019-0305-5>
- Catalán J, Rydman E, Aimonen K, Hannukainen KS, Suhonen S, Vanhala E, Moreno C, Meyer V, Perez DD, Sneek A, Forsström U, Højgaard C, Willemoes M, Winther JR, Vogel U, Wolff H, Alenius H, Savolainen KM, Norppa H (2017) Genotoxic and inflammatory effects of nanofibrillated cellulose in murine lungs. *Mutagenesis* 32:23–31. <https://doi.org/10.1093/mutage/gew035>
- Donaldson K, Poland CA, Murphy FA, MacFarlane M, Chernova T, Schinwald A (2013) Pulmonary toxicity of carbon nanotubes and asbestos—similarities and differences. *Adv Drug Deliv Rev* 65:2078–2086. <https://doi.org/10.1016/j.addr.2013.07.014>
- Endes C, Camarero-Espinosa S, Mueller S, Foster EJ, Petri-Fink A, Rothen-Rutishauser B, Weder C, Clift MJ (2016) A critical review of the current knowledge regarding the biological impact of nanocellulose. *J Nanobiotechnol* 14:78. <https://doi.org/10.1186/s12951-016-0230-9>
- Farcas MT, Kisin ER, Menas AL, Gutkin DW, Star A, Reiner RS, Yanamala N, Savolainen K, Shvedova AA (2016) Pulmonary exposure to cellulose nanocrystals caused deleterious effects to reproductive system in male mice. *J Toxicol Environ Health A* 79:984–997. <https://doi.org/10.1080/15287394.2016.1211045>
- Fujita K, Fukuda M, Endoh S, Maru J, Kato H, Nakamura A, Shinohara N, Uchino K, Honda K (2015) Size effects of single-walled carbon nanotubes on in vivo and in vitro pulmonary toxicity. *Inhal Toxicol* 27(4):207–223. <https://doi.org/10.3109/08958378.2015.1026620>
- Fujita K, Fukuda M, Endoh S, Maru J, Kato H, Nakamura A, Shinohara N, Uchino K, Honda K (2016) Pulmonary and pleural inflammation after intratracheal instillation of short single-walled and multi-walled carbon nanotubes. *Toxicol Lett* 257:23–37. <https://doi.org/10.1016/j.toxlet.2016.05.025>
- Fujita K, Obara S, Maru J, Endoh S (2020) Cytotoxicity profiles of multi-walled carbon nanotubes with different physico-chemical properties. *Toxicol Mech Methods* 30:477–489. <https://doi.org/10.1080/15376516.2020.1761920>
- Fulkerson PC, Rothenberg ME (2013) Targeting eosinophils in allergy, inflammation and beyond. *Nat Rev Drug Discovery* 12:117–129. <https://doi.org/10.1038/nrd3838>
- Gordon SC, Butala JH, Carter JM, Elder A, Gordon T, Gray G, Sayre PG, Schulte PA, Tsai CS, West J (2014) Workshop report: strategies for setting occupational exposure limits for engineered nanomaterials. *Regul Toxicol Pharmacol* 68:305–311. <https://doi.org/10.1016/j.yrtph.2014.01.005>
- Hadrup N, Knudsen KB, Berthing T, Wolff H, Bengtson S, Kofoed C, Espersen R, Højgaard C, Winther JR, Willemoes M, Wedin I, Nuopponen M, Alenius H, Norppa H, Wallin H, Vogel U (2019) Pulmonary effects of nanofibrillated celluloses in mice suggest that carboxylation lowers the inflammatory and acute phase responses. *Environ Toxicol Pharmacol* 66:116–125. <https://doi.org/10.1016/j.etap.2019.01.003>
- Honda K, Naya M, Takehara H, Kataura H, Fujita K, Ema M (2017) A 104-week pulmonary toxicity assessment of long and short single-wall carbon nanotubes after a single intratracheal instillation in rats. *Inhalation Toxicol* 29(11):471–482. <https://doi.org/10.1080/08958378.2017.1394930>
- Ihrle MD, Taylor-Just AJ, Walker NJ, Stout MD, Gupta A, Richey JS, Hayden BK, Baker GL, Sparrow BR, Duke KS, Bonner JC (2019) Inhalation exposure to multi-walled carbon nanotubes alters the pulmonary allergic response of mice to house dust mite allergen. *Inhalation Toxicol* 31:192–202. <https://doi.org/10.1080/08958378.2019.1643955>
- Ilves M, Vilske S, Aimonen K, Lindberg HK, Pesonen S, Wedin I, Nuopponen M, Vanhala E, Højgaard C, Winther JR, Willemoes M, Vogel U, Wolff H, Norppa H, Savolainen K, Alenius H (2018) Nanofibrillated cellulose causes acute pulmonary inflammation that subsides within a month. *Nanotoxicology* 12:729–746. <https://doi.org/10.1080/17435390.2018.1472312>
- Inoue K, Yanagisawa R, Koike E, Nishikawa M, Takano H (2010) Repeated pulmonary exposure to single-walled carbon nanotubes exacerbates allergic inflammation of the airway: possible role of oxidative stress. *Free Radic Biol Med* 48:924–934. <https://doi.org/10.1016/j.freeradbiomed.2010.01.013>
- International Organization for Standardization (2017) ISO/TS 20477:2017—Standard terms and their definition for cellulose nanomaterial. International Organization for Standardization, Geneva, Switzerland
- Isogai A (2013) Wood nanocelluloses: fundamentals and applications as new bio-based nanomaterials. *J Wood Sci* 59:449–459. <https://doi.org/10.1007/s10086-013-1365-z>
- Isogai A, Saito T, Fukuzumi H (2011) TEMPO-oxidized cellulose nanofibers. *Nanoscale* 3:71–85. <https://doi.org/10.1039/c0nr00583e>
- Kangas H (2013) Cellulose nanofibrils: a class of materials with unique properties and many potential applications. In: Postek MT, Moon RJ, Rudie AW, Bilodeau MA (eds) *Production and applications of cellulose nanomaterials*. TAPPI Press, pp 169–174
- Kasai T, Umeda Y, Ohnishi M, Mine T, Kondo H, Takeuchi T, Matsumoto M, Fukushima S (2016) Lung carcinogenicity of inhaled multi-walled carbon nanotube in rats. *Part Fibre Toxicol* 13:53. <https://doi.org/10.1186/s12989-016-0164-2>
- Knudsen KB, Kofoed C, Espersen R, Højgaard C, Winther JR, Willemoes M, Wedin I, Nuopponen M, Vilske S, Aimonen K, Weydahl IE, Alenius H, Norppa H, Wolff H, Wallin H, Vogel U (2015) Visualization of nanofibrillar cellulose in biological tissues using a biotinylated carbohydrate binding module of β -1,4-Glycanase. *Chem Res Toxicol*

- 28:1627–1635. <https://doi.org/10.1021/acs.chemrestox.5b00271>
- Kobayashi T, Oshima Y, Tsubokura Y, Kayashima T, Nakai M, Imatanaka N, Kano H, Senoh H, Suzuki M, Kondo H, Fukushima S (2019) Standardization of intratracheal instillation study of manufactured nanomaterials. In: Takebayashi T, Landsiedel R, Gamo M (eds) *In vivo* inhalation toxicity screening methods for manufactured nanomaterials. Springer, Singapore, pp 107–122
- Ma-Hock L, Treumann S, Strauss BS, Luizi F, Mertler M, Wiench K, Gamer AO, van Ravenzwaay B, Landsiedel R (2009) Inhalation toxicity of multiwall carbon nanotubes in rats exposed for 3 months. *Toxicol Sci* 112:468–481. <https://doi.org/10.1093/toxsci/kfp146>
- Morimoto Y, Hirohashi M, Ogami A, Oyabu T, Myojo T, Todoroki M, Yamamoto M, Hashiba M, Mizuguchi Y, Lee BW, Kuroda E, Shimada M, Wang WN, Yamamoto K, Fujita K, Endoh S, Uchida K, Kobayashi N, Mizuno K, Inada M, Tao H, Nakazato T, Nakanishi J, Tanaka I (2012) Pulmonary toxicity of well-dispersed multi-wall carbon nanotubes following inhalation and intratracheal instillation. *Nanotoxicology* 6:587–599. <https://doi.org/10.3109/17435390.2011.594912>
- Muller J, Huaux F, Moreau N, Misson P, Heilier JF, Delos M, Arras M, Fonseca A, Nagy JB, Lison D (2005) Respiratory toxicity of multi-wall carbon nanotubes. *Toxicol Appl Pharmacol* 207:221–231. <https://doi.org/10.1016/j.taap.2005.01.008>
- Murphy FA, Poland CA, Duffin R, Al-Jamal KT, Ali-Boucetta H, Nunes A, Byrne F, Prina-Mello A, Volkov Y, Li S, Mather SJ, Bianco A, Prato M, Macnee W, Wallace WA, Kostarelos K, Donaldson K (2011) Length-dependent retention of carbon nanotubes in the pleural space of mice initiates sustained inflammation and progressive fibrosis on the parietal pleura. *Am J Pathol* 178(6):2587–2600. <https://doi.org/10.1016/j.ajpath.2011.02.040>
- Nechyporchuk O, Belgacem MN, Pignon F (2016a) Current progress in rheology of cellulose nanofibril suspensions. *Biomacromol* 17:2311–2320. <https://doi.org/10.1021/acs.biomac.6b00668>
- Nechyporchuk O, Belgacem MN, Bras J (2016b) Production of cellulose nanofibrils: a review of recent advances. *Ind Crops Prod* 93:2–25. <https://doi.org/10.1016/j.indcrop.2016.02.016>
- Ogura I, Kotake M, Kuboyama T, Kajihara H (2020) Measurements of cellulose nanofiber emissions and potential exposures at a production facility. *NanoImpact*. <https://doi.org/10.1016/j.impact.2020.100273>
- Park EJ, Khaliullin TO, Shurin MR, Kisin ER, Yanamala N, Fadeel B, Chang J, Shvedova AA (2018) Fibrous nanocellulose, crystalline nanocellulose, carbon nanotubes, and crocidolite asbestos elicit disparate immune responses upon pharyngeal aspiration in mice. *J Immunotoxicol* 15:12–23. <https://doi.org/10.1080/1547691X.2017.1414339>
- Pauluhn J (2010) Subchronic 13-week inhalation exposure of rats to multiwalled carbon nanotubes: toxic effects are determined by density of agglomerate structures, not fibrillar structures. *Toxicol Sci* 113:226–242. <https://doi.org/10.1093/toxsci/kfp247>
- Pitkänen M, Kangas H, Laitinen O, Sneek A, Lahtinen P, Peresin MS, Niinimäki J (2014) Characteristics and safety of nano-sized cellulose fibrils. *Cellulose* 21:3871–3886. <https://doi.org/10.1007/s10570-014-0397-x>
- Sai T, Fujita K (2020) A review of pulmonary toxicity studies of nanocellulose. *Inhalation Toxicol* 32:231–239. <https://doi.org/10.1080/08958378.2020.1770901>
- Sai T, Maru J, Obara S, Endoh S, Kajihara H, Fujita K (2020) Screening of preservatives and evaluation of sterilized cellulose nanofibers for toxicity studies. *J Occup Health* 62(1):e12176. <https://doi.org/10.1002/1348-9585.12176>
- Sharma A, Thakur M, Bhattacharya M, Mandal T, Goswami S (2019) Commercial application of cellulose nano-composites—a review. *Biotechnol Rep* 15:e00316. <https://doi.org/10.1016/j.btre.2019.e00316>
- Shatkin JA, Ong KJ, Ede JD, Wegner TH, Goergen M (2016) Toward cellulose nanomaterial commercialization: knowledge gap analysis for safety data sheets according to the globally harmonized system. *TAPPI J* 15:425–437. <https://doi.org/10.32964/TJ15.6.425>
- Shatkin JA, Kim B (2015) Cellulose nanomaterials: life cycle risk assessment, and environmental health and safety roadmap. *Environ Sci Nano* 2:477–499. <https://doi.org/10.1039/C5EN00059A>
- Shvedova AA, Kisin ER, Yanamala N, Farcas MT, Menas AL, Williams A, Fournier PM, Reynolds JS, Gutkin DW, Star A, Reiner RS, Halappanavar S, Kagan VE (2016) Gender differences in murine pulmonary responses elicited by cellulose nanocrystals. *Part Fibre Toxicol* 13:28. <https://doi.org/10.1186/s12989-016-0140-x>
- Silva RM, Doudrick K, Franzi LM, TeeSy C, Anderson DS, Wu Z, Mitra S, Vu V, Dutrow G, Evans JE, Westerhoff P, Van Winkle LS, Raabe OG, Pinkerton KE (2014) Instillation versus inhalation of multiwalled carbon nanotubes: exposure-related health effects, clearance, and the role of particle characteristics. *ACS Nano* 8:8911–8931. <https://doi.org/10.1021/nn503887r>
- Trache D, Tarchoun AF, Derradji M, Hamidon TS, Masruchin N, Brosse N, Hussin MH (2020) Nanocellulose: from fundamentals to advanced applications. *Front Chem* 8:392. <https://doi.org/10.3389/fchem.2020.00392>
- Treumann S, Ma-Hock L, Gröters S, Landsiedel R, van Ravenzwaay B (2013) Additional histopathologic examination of the lungs from a 3-month inhalation toxicity study with multiwall carbon nanotubes in rats. *Toxicol Sci* 134:103–110. <https://doi.org/10.1093/toxsci/kft089>
- Ventura C, Pinto F, Lourenço AF, Ferreira PJT, Louro H, Silva MJ (2020) On the toxicity of cellulose nanocrystals and nanofibrils in animal and cellular models. *Cellulose* 27:5509–5544. <https://doi.org/10.1007/s10570-020-03176-9>

Publisher's Note Springer Nature remains neutral with regard to jurisdictional claims in published maps and institutional affiliations.